Journal of The Electrochemical Society, **159** (3) A253-A258 (2012)
0013-4651/2012/159(3)/A253/6/$28.00 © The Electrochemical Society

In Situ XRD Investigation and Thermal Properties of Mg Doped $LiCoO_2$ for Lithium Ion Batteries

Ri-Zhu Yin,[a,z] Yang-Soo Kim,[b,z] Se-Jong Shin,[a] Inho Jung,[a] Jeom-Soo Kim,[c] and Soon-Ki Jeong[d]

[a]*R&D Center, Samsung SDI Co. Ltd., Chungnam-do 446-577, Korea*
[b]*Suncheon Center, Korea Basic Science Institute, Suncheon 540-742, Korea*
[c]*Advanced Batteries Research Center, Korea Electronic Technology Institute, Gyeonggi-do 463-816, Korea*
[d]*Department of Chemical Engineering, Soonchunhyang University, Chungnam 336-745, Korea*

Mg-doped $LiCoO_2$ is synthesized by a solid-state reaction as a positive electrode material for lithium-ion batteries. The uniphase solid solution is confirmed by X-ray diffraction (XRD) and Rietveld refinements. The structural changes during charging are calculated theoretically by the general gradient approximation (GGA) *ab initio* method. A blue-pouched single half-cell was used to collect in-situ XRD patterns while the cell charged and discharged in the range of 3.0∼4.5 V. Good structural reversibility and symmetric cell parameter changes were observed during charging and discharging. The 'W' and inverse 'W' shapes of the a- and c-cell parameter changes, respectively, were also observed. The cell volume changes show an inverse 'W' shape. No large hysteresis occurs during the changes in the cell parameters during the charging-discharging process. The thermally stable Mg-doped $LiCoO_2$ is confirmed by differential scanning calorimetry (DSC) and evolved gas analysis-mass spectrometry (EGA-MS).
 [DOI: 10.1149/2.006203jes]

Manuscript submitted October 7, 2011; revised manuscript received November 21, 2011. Published January 3, 2012.

In recent years, lithium-ion battery technology has enjoyed great commercial success due to the rapid achievement of portable electronics, including the cellular phone and the notebook PC. In the meantime, researchers continue to achieve better performance, higher capacity, a longer cycle life and develop less expensive electrode materials in their efforts to ensure lasting success in this area.[1–3]

Lithium-ion batteries presently adopt lithium transition metal oxides as a positive electrode material and graphite as a negative electrode material.[4] It is well known that lithium-ion batteries offer a higher energy density, higher average voltage, and a higher power density than existing rechargeable batteries such as those based on Ni-MH or Ni-Cd.

Much work has gone into improving the capacity of $LiCoO_2$. One effective way to improve the capacity is to increase the charging voltage. Easily reversible and stable structural changes as the cell charges and discharges are required for such an improvement. Metal-doped $LiCoO_2$ is well known as a structurally stable positive electrode material, as has been reported in several papers.[5–7]

Mg is a nontoxic and easily obtainable element. It also offers improved cycling stability, as reported by Stoyanova et al.,[8] because the Mg element can stabilize the crystal structure. A small amount of Mg-doped $LiCoO_2$ should be the best positive electrode candidate for a high-voltage lithium-ion battery system.

In the present work, a theoretical ab initio calculation study was conducted using the CASTEP program package, based on the density-functional-theory pseudo-potential plane wave method and the general gradient approximation (GGA) exchange and correlation functional, to obtain the structural parameters. The structural properties were characterized by XRD Rietveld refinement and extended X-ray absorption fine structure (EXAFS) analysis. The thermal stability was also determined by DSC and evolved gas analysis-mass spectrometry. The structural change mechanisms of the charge and discharge were investigated by in-situ XRD analysis.

Experimental

Powder preparation.— Mg-doped $LiCoO_2$ was prepared by thoroughly mixing stoichiometric amounts of Co_3O_4 (>99.9% pure), Li_2CO_3, and $MgCO_3$. The mixed precursors were calcinated at 800°C for 6 hours and then cooled. The calcinated powders were ground and mixed well before finally being sintered at 850°C for 10 hours. All experiments were carried out in an N_2 inert atmosphere.

The maximum Mg content was set at 2 mol% for reasons of capacity. Within this limitation, Mg-doped $LiCoO_2$ was synthesized at several different substituting levels, 0, 1.0, 1.5 and 2.0 mol%. The particle size and morphology among the samples were kept close to each other to minimize the effect of the size and morphology on the thermal and electrochemical properties.

Structural characterization.— The XRD patterns of the powder samples were recorded by a Philips X'pert X-ray diffractometer at room temperature. The XRD data were analyzed using Rietveld's powder diffraction profile-fitting technique with Cerius 2 (Version 4.8.1, with DBWS, S.G. Inc.) to determine the crystallographic information, in this case the lattice parameters and atomic coordinates.

In-situ XRD patterns were collected on the BL5A High Flux X-ray scattering beam line of the Pohang Light Source. To minimize the collecting time, an MAR3450 image plate was used to record the XRD patterns. The collecting time was 40 seconds per scan with an 18keV mono-beam, and the storage ring current was maintained at 120–190 mA and 2.5 GeV.

The Co K-edge X-ray absorption spectra (XAS) were recorded on the BL7C beam line of the Pohang Light Source with a storage ring current of 120–190 mA at 2.5 GeV. A Si(311) double-crystal monochromator was used to change the energy from 2 to 23 keV. The XAS spectra were measured in transmission mode and the electrode thickness was controlled to obtain high-quality spectra.

Electrochemical characterization.— An in-situ pouch cell was made in the lab and the electrochemical charge and discharge process was performed with a Wonatech potentiostat WPG1000. The positive electrode consisted of the active material, poly(vinylidene difluoride) (PVDF), and conducting additives. 1.15 mol dm^{-3} (M) $LiPF_6$ in a mixture of ethylene carbonate (EC) / ethylmethyl carbonate (EMC) / diethyl carbonate (DEC) with a weight ratio of 3:6:1 was used as the electrolyte. For the electrochemical evaluation, the assembled cells were cycled under a constant current condition at a 0.1 C rate with a voltage window of 4.5–3.0 V at room temperature. All potentials were referred to as volts vs. Li/Li^+.

Computational procedure.— CASTEP (Materials Studio CASTEP, Accelrys Inc., San Diego, 2002) is a density-functional (DFT) plane-wave pseudo-potential method. The ab initio calculations were performed using the GGA throughout, which provides a more accurate overall description of the electronic subsystem than does the local density approximation (LDA). In particular, PBE

[z] E-mail: kimyangsoo@kbsi.re.kr; rzyin@yahoo.com

exchange-correlation functions were used in the calculation.[9] These are the default function in GGA CASTEP calculations.

The electronic structure was calculated by the parameterization of all atoms of the crystal using ultra-soft pseudo-potentials for the core electrons. The geometry optimization of the Mg-doped $LiCoO_2$ structure was performed with a basis set cutoff of 340 eV. This is sufficient to obtain good geometry optimization of the structure and gives accurate results for the electronic structure.

Thermal characterization.— Thermal characterization of the $LiCoO_2$ and the Mg-doped $LiCoO_2$ was carried out using a TA Instruments DSC 2910 differential scanning calorimeter. A pressure cell (a high-pressure pan made from stainless steel) was used as a sample pan to prevent any leakage that might occur during the measurement.

The measurement was carried out in an N_2 atmosphere between 50 and 360°C at a heating rate of 10°C min^{-1}. For the measurement, positive electrodes were charged to 4.5 V at a constant current of 0.5 C in coin-type cells. After charging, the cells were disassembled in a dry room. The cell voltage was checked before disassembly and after to monitor any shorting that may have occurred during the cell disassembly process. The positive electrode was carefully scraped from the aluminum current collector and loaded onto a stainless steel pan. The stainless steel pan was sealed without electrolyte insertion and transferred immediately to the DSC instrument.

To investigate the structural stability, the EGA-MS technique was used at temperatures between 120°C and 420°C at a heating rate of 10°C min^{-1}. EGA-MS consists of a furnace type pyrolyzer (PY-2020iD, Frontier Lab., Japan) and a GC oven (6890N, Agilent Technologies, USA) coupled to a mass-selective detector (MSD) (5973 inert GC/MS, Agilent Technologies, USA) by a short 2.5 m deactivated EGA capillary tube (UADTM-2.5N, Frontier Lab., Japan). This is a simple thermal analytical technique in which the furnace (pyrolyzer) is programmatically heated and the evolved gases produced from the sample are recorded on-line by the MSD. The MSD provides the mass spectral information of the decomposition components of the samples.

In the EGA-MS experiments, a 20 mg sample was placed in the pan and heated to 420°C at a heating rate of 10°C min^{-1} under a 1 mL min^{-1} helium flow. The temperature of the capillary tube was held at 300°C.

Results and Discussion

Powder morphology.— All samples in this study had a round morphology, as shown in Fig. 1. Mg substitution did not have an influence on the powder morphology. There was no difference between the primary and secondary particles (single-particle powder). In an effort to optimize the particle size, several different sizes of particles were examined. The 20 μm sample showed the best performance in terms of the cycle life. The average particle size of the obtained samples was around 16–17 μm. The surface of the powder was relatively clean and smooth.

Structural properties.— All samples were good solid solutions without any impurities. The Rietveld refinement of the model resulted in a satisfactory fit to the overall profile. The best-fit of the XRD pattern for the $LiCoO_2$ is shown in Fig. 2. The Mg-doped $LiCoO_2$ showed a pattern similar to that of $LiCoO_2$.

The refinement processes were carried out with several variations. These included baseline correction, zero correction, and variation of the cell parameters, scale factor, and temperature factor. All compounds were assigned to the hexagonal system with the R-3m space group.

The a- and c-cell parameters increased with the Mg content as the larger Mg^{2+} ions replaced the smaller Co^{3+} ions. The cell parameters are listed in Table I. The oxygen coordinate z was kept at 0.260 for all samples, which means that Mg substitution did not affect the oxygen position. The Rietveld analysis confirms that Mg prefers to substitute for the Co position instead of the Li position.

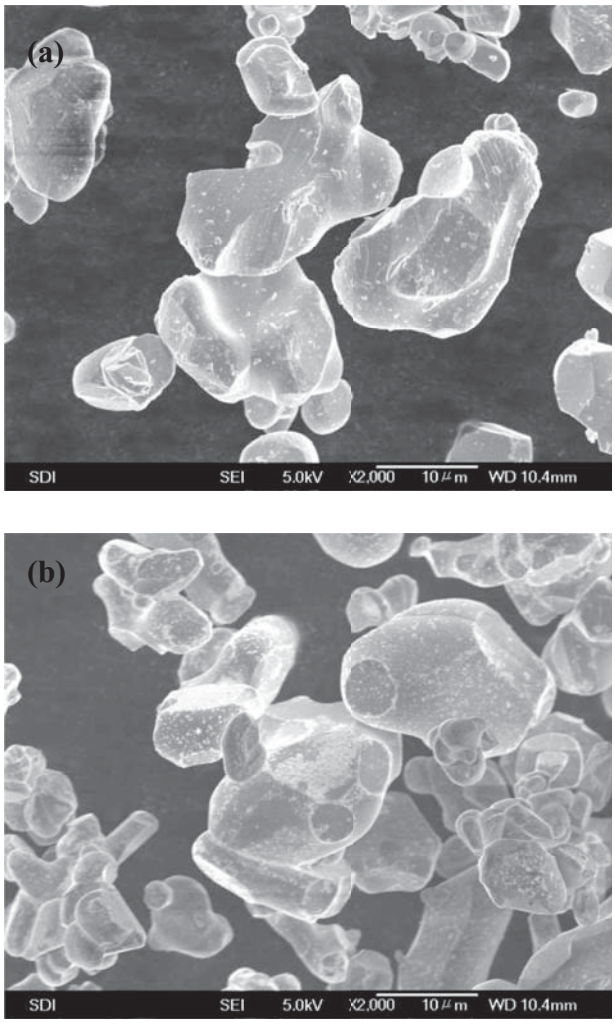

Figure 1. The SEM image of the (a) $LiCoO_2$ and (b) Mg 1% doped $LiCoO_2$.

The EXAFS data of the Mg-doped $LiCoO_2$ powder were analyzed with the UWXAFS package. The representative best-fit result in the R-space is shown in Fig. 3. All samples had six oxygen atoms coordinated

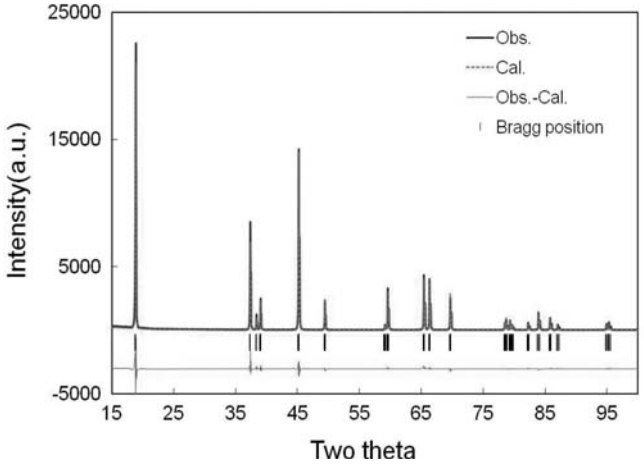

Figure 2. Rietveld refinements of XRD pattern for $LiCoO_2$.

Table I. Cell parameters of the Mg doped $LiCoO_2$.

y value in $LiMg_yCo_{1-y}O_{2-y/2}$	S.G.	Cell parameters a (Å)	c (Å)	V (Å^3)
0.00	R-3m	2.815	14.046	96.385
0.01	R-3m	2.817	14.056	96.581
0.02	R-3m	2.818	14.063	96.721

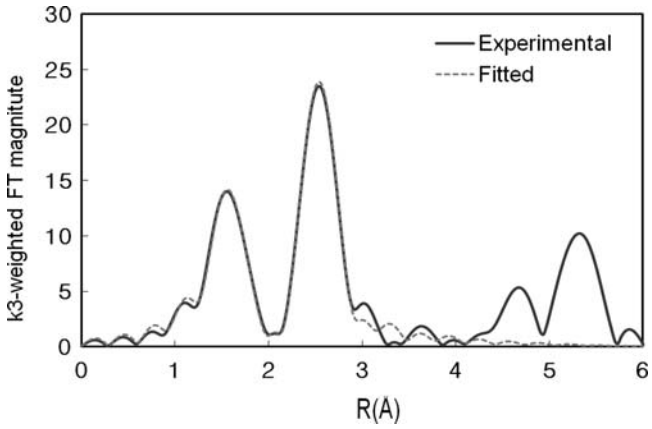

Figure 3. The best-fitted EXAFS spectrum of Mg 1% doped $LiCoO_2$ in R-space.

with Co and had a bond length identical to that of Co-O. Fitting was carried out for the first Co-O shell and second Co-Co shell.

The Co-O and Co-Co bond lengths increased with the Mg substituted content, as shown in Table II. These results are in good agreement with the bond length and cell parameter changes determined from the XRD analysis. The Debye-Waller factor remained nearly unchanged with the Mg content due to there not being enough Mg substituted to affect the static ordering state or the oxygen deficiency.

In-situ XRD and computational results.— The laboratory-created half-cell sealed in a blue pouch showed feasible electrochemical behavior. The 4.5 V charge capacity is 184 mAh g^{-1}, and the discharge capacity is 174 mAh g^{-1} at a 0.1 C rate. The XRD patterns were varied reversibly during the charge and discharge processes, as shown in Fig. 4.

The lattice parameters are indexed using a DICVOL02 program. The a and c parameter changes are shown in Fig. 5. During the calculation of the cell parameters by the least squares method, the uncertainty of the peak position of the recorded pattern was noted to be much smaller than the uncertainty of the conventional XRD measured peak position. This reduction in the uncertainty could yield more reliable and accurate values for indexed cell parameters.

The monoclinic phase of $LiCoO_2$ was found at about 4.2 V, as originally proposed by Amatucci.[10] Mg doping can improve the stability of the structural properties and suppress the formation of the monoclinic phase.[5] In this system, 1% Mg doping was enough to stabilize the crystal structure, and no phase transition from hexagonal to monoclinic was noted in the range 3.0 to 4.5 V.

The a parameter was found to decrease as the state of charge increased. The starting a parameter was 2.814 Å. This value decreased to 2.805 Å upon charging and then increased to 2.807 Å upon further charging. The c parameter showed the opposite behavior: with an increase in the state of charge, the c parameter increased from 14.05 Å to 14.43 Å and then decreased to 14.33 Å. The increased c parameter can be attributed to the lattice repulsion which occurred due to the weaker Li-ion bridge.

The unit cell volume changes are follow the c parameter changes because the dominant changes in this system were c parameter changes. The a parameter only changed by about 0.009 Å during the charge and discharge process. This amount of change was much smaller than that of the c parameter, which changed by about 0.38 Å during the charge and discharge process. The unit cell volume increased upon charging, from 96.27 Å to 98.30 Å, after which it de-

Table II. The EXAFS fitting results of Mg doped $LiCoO_2$.

y value in $LiMg_yCo_{1-y}O_{2-y/2}$	R(EXAFS) (Å) Co-O	R(EXAFS) (Å) Co-Co	R(XRD) (Å) Co-O	R(XRD) (Å) Co-Co	σ^2	r-fit
0.000	1.927	2.825	1.923	2.815	0.003	0.006
0.010	1.929	2.828	1.927	2.817	0.003	0.002
0.015	1.930	2.830	1.934	2.818	0.003	0.001

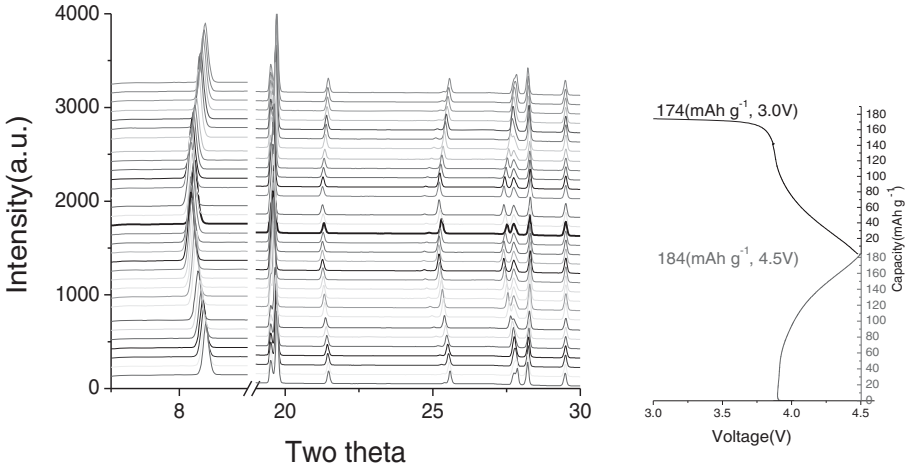

Figure 4. The in-situ XRD pattern's variation of Mg 1% doped $LiCoO_2$ during charge and discharge process. The synchrotron source X-ray wavelength is 0.686 Å.

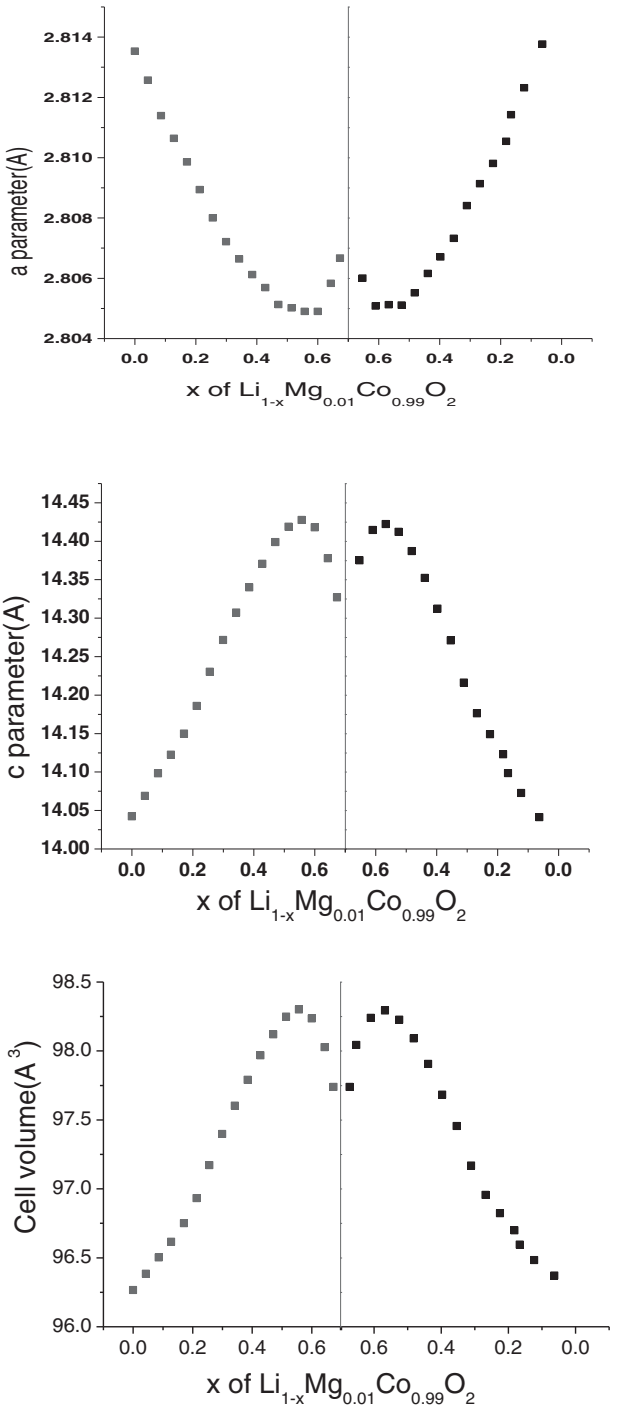

Figure 5. The cell a, c parameters, and cell volume changes during charge and discharge.

creased to 97.74 Å. The maximum volume changes were 2.1%. The minimum value of the a parameter, the maximum of the c parameter and the maximum of the cell volume were noted to occur at 4.28 V, at which point the composition is $Li_{0.557}Mg_{0.01}Co_{0.99}O_2$.

To compare the bare $LiCoO_2$, the cell parameter changes of Mg-doped $LiCoO_2$ are more smaller than the bare $LiCoO_2$. In the bare $LiCoO_2$ sample, the maximum and minimum of the a parameter values are changed from 2.814 Å to 2.804 Å and the c parameter values are changed from 14.05 Å to 14.45 Å in the 1st charge and discharge. We envisage that Mg-doping induced octahedron expansion stabilizes the Co^{3+} state, so the cell parameter changes are relatively smaller than

Table III. The structure optimized lattice parameter calculated with CASTEP.

$Li_{1-x}Mg_{0.01}Co_{0.99}O_2$	a (%)	c (%)	V (%)
x = 0	100	100	100
x = 0.33	99.42595	101.412	113.5217
x = 0.66	99.18625	103.4042	111.8734
x = 1	99.18595	91.08808	111.5933

the bare sample.[11] It is also consist with the result of Delma's group.[5] It is obvious that the stable structure can increase the thermal stability.

The lattice parameter changes were consistent with the calculated results. The structurally optimized theoretical calculation results are listed in Table III. The smallest a parameter was noted at approximately x = 0.6, and the largest c parameter was recorded at about x = 0.6 in $Li_{1-x}Mg_{0.01}Co_{0.99}O_2$. These results are in good agreement with the in-situ XRD results.

The stable structure also improves the cycleability of electrode as shown in Fig. 6. The 2016 coin type cell discharge capacity of $LiCoO_2$ showed higher than Mg-doped $LiCoO_2$ at 1 C while both samples showed identical capacity (183 mAh/g) at 0.1 C. The capacity of $LiCoO_2$ is kept 81% after 50 cycles at 1 C rate and the capacity of Mg-doped $LiCoO_2$ is kept 85% after 50 cycles at 1 C rate. The cycling performance is very satisfactory as already reported elsewhere.[5]

Thermal properties.— The thermal behavior of $LiCoO_2$ and Mg 1% doped $LiCoO_2$ were characterized by DSC. Both samples were charged with a constant current followed by a constant voltage level to 4.3 V and 4.5 V. Battery safety becomes a critical issue when the battery manufacturer chooses a high-voltage method to develop higher energy capacity. The possible safety problems are shown in Fig. 7a when the charge voltage is increased from 4.3 (current system) to 4.5 V (higher voltage system). As the charge voltage increases, the initial exothermic peak is shifted down from 220 to 180°C and the two main peaks (4.3 V) are merged to create a single main peak (4.5 V). The temperature of the initial exothermic reaction (4.3 V) was found to agree well with values determined in a previous report.[12] These instances of exothermic heat generation are attributed to sample decomposition accompanied by oxygen evolution.[13–15]

The initial exothermic regime of Mg-doped $LiCoO_2$ moved by 20°C compared to that of $LiCoO_2$ (220 → 240°C) at 4.3 V. $LiCoO_2$

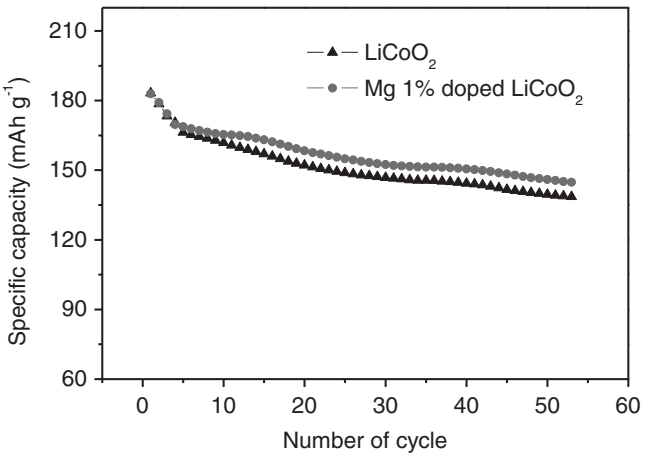

Figure 6. The cycling performance of Li / $LiCoO_2$ and Li / Mg 1% doped $LiCoO_2$ electrochemical cells. During the galvanostatic cycle at room temperature, the current was varied (0.1 C, 0.2 C, and 0.5 C) for first 3 cycles. 1 C current was kept for further cycles up to 50 cycles.

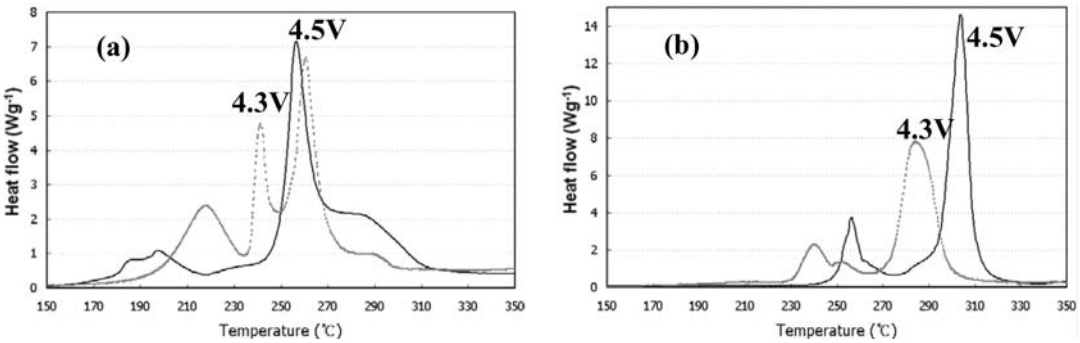

Figure 7. DSC measurement of (a) $LiCoO_2$ (b) Mg 1% doped $LiCoO_2$ which was charged to different voltage (4.3 V and 4.5 V). Samples were heated to 350°C with heating rate of 10°C min^{-1}.

showed two main peaks at around 250°C, while Mg-doped $LiCoO_2$ showed one main exothermic peak at around 290°C when the samples were charged to 4.5 V as shown in Fig. 7b. 1 mol% Mg substitution was enough to improve the thermal stability significantly by increasing the decomposition temperature. The enhanced thermal stability is attributed to the structural stability resulting from Mg substitution. The main difference between the $LiCoO_2$ and the Mg-doped $LiCoO_2$ is the direction of profile shifting as the charge voltage increases from 4.3 V to 4.5 V. The thermal profile of the $LiCoO_2$ shifts to a lower temperature, whereas that of the Mg-doped $LiCoO_2$ shifts to a higher temperature. When the lithium is removed from the active material during charging, its structure becomes unstable. The increased concentration of Co^{4+} may catalyze an electrolyte / oxygen reaction.

Consequently, it was found that the thermal stability deteriorates in general when the sample is charged to a higher voltage (less lithium in the structure). It is not fully understood how the thermal stability of the system can improve under a lower lithium concentration with a higher oxidation state. Further study of this issue is in progress to determine the cause of this behavior more thoroughly.

To compare the DSC profiles of $LiCoO_2$ and Mg-doped $LiCoO_2$ charged to 4.5 V, the initial and main exothermic peaks were shifted to higher temperatures by 80 and 60°C, respectively. The temperature of the initial exothermic reaction is more critical to the safety feature of the battery system than is the temperature of the main exothermic reaction.

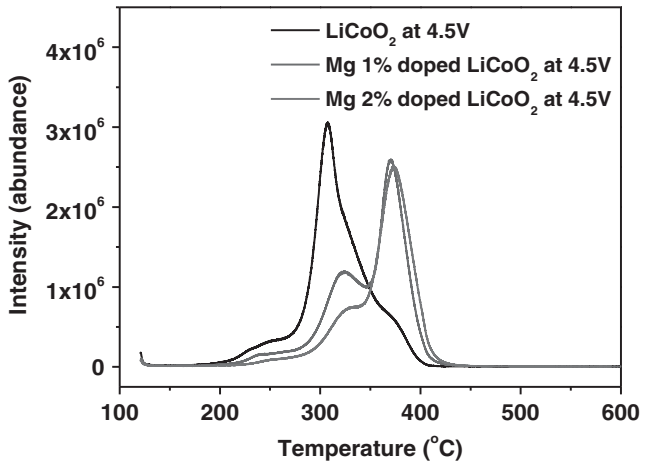

Figure 8. EGA-MS curves of $LiCoO_2$ and Mg doped $LiCoO_2$ charged to 4.5 V. Samples were heated to 450°C with heating rate of 10°C min^{-1}. The detected gas is O_2, the main peaks are shifted higher temperature with increasing doped Mg contents.

The thermal reaction scheme for a full cell using $LiCoO_2$ is proposed as follows: (i) thermal breakdown of the solid electrolyte interface (SEI) on the negative electrode, (ii) thermal decomposition reaction of the electrolyte with the negative electrode material, (iii) thermal decomposition of the positive electrode material followed by a chemical reaction with the electrolyte, and, finally, (iv) the reaction of the PVDF binder with the lithiated negative electrode (Li_xC_6).[16]

Among these steps, the first step (i) initiates the thermal runaway reaction at a relatively low temperature (~120°C). If $LiCoO_2$ is used as an active material for the positive electrode, the interval between the SEI breakdown and the decomposition of the positive electrode is too short to dissipate the heat generated by the first step because the onset of the decomposition of the positive electrode occurs at around 180°C. With Mg-doped $LiCoO_2$, this problem is mitigated. There is enough of a temperature difference (130°C) between step (i) and the decomposition of the positive electrode. This will allow enough time to dissipate the generated heat because the onset of the decomposition of the positive electrode is shifted significantly to a higher temperature (60°C) with the use of Mg-doped $LiCoO_2$.

The main peak of DSC is associated with oxygen evolution. Oxygen evolution may cause cell swelling, which critically affects cell cycle performance due to the increasing resistance. To investigate O_2 evolution, EGA-MS measurements were taken. The O_2 evolved data are shown in Fig. 8.

It is clear that the O_2 evolution of Mg-doped $LiCoO_2$ is more stable than that of $LiCoO_2$. The starting onset point is shifted to a higher temperature with an increase in the doped Mg content in the Mg-doped $LiCoO_2$ system.

The $LiCoO_2$ onset point is 206°C, the Mg-doped $LiCoO_2$ shifts to a higher temperature, the onset point of Mg 1% doped $LiCoO_2$ is 217°C, and that of Mg 2% doped $LiCoO_2$ is 226°C. The amount of O_2 evolution, which is produced by positive electrode decomposition, can be described by the peak area of the EGA-MS spectrum. It is clearly observable that the main peak is shifted to a higher temperature of about 90°C in the Mg-doped $LiCoO_2$ system.

The decreased area of the first and second peaks can be observed for Mg-doped $LiCoO_2$; the Mg 2% doped $LiCoO_2$ shows a smaller peak area than that of the Mg 1% doped $LiCoO_2$. This discrepancy means that with an increase in the Mg content in Mg-LCO, the sample should exhibit stable structural properties and restricted O_2 evolution.

Conclusions

Mg-doped $LiCoO_2$ was synthesized by a conventional solid-state reaction. The compounds were assigned to a hexagonal system with an R-3m space group according to XRD Rietveld refinement. The lattice parameters were found to increase with an increase in the Mg doping content. The bond-length of Co-O was also found to increase with an increase in the Mg doping content. These determinations were confirmed by XAS spectrum fitting.

The Mg doping increases the thermal stability of the positive electrode materials. The exothermic peak is shifted to a higher temperature in Mg-doped $LiCoO_2$ as compared to $LiCoO_2$. The Mg, substituting for the Co ion, will increase the stability of the active materials and increase the safety of Li-ion batteries.

Accurate lattice parameter calculations were performed with in-situ XRD spectra that were measured with an image plate equipped synchrotron sources. The a parameter was found to decrease with an increase in the x value (charge) in $Li_{1-x}Mg_{0.01}Co_{0.99}O_2$, and the c parameter was found to increase with an increase in the x value (charge) in $Li_{1-x}Mg_{0.01}Co_{0.99}O_2$. Both the smallest a parameter and the maximum c parameter value arose at $x = 0.6$ in $Li_{1-x}Mg_{0.01}Co_{0.99}O_2$, which is consistent with the value calculated using the GGA method by CASTEP. The a and c parameter changes show good reversibility during the charge and discharge process.

Acknowledgments

This work was supported by SDI Co. The authors also thank So-Hyun Hur and other members of the Cathode Group in the Energy Laboratory for their fruitful technical discussions and experimental support. The in-situ XRD and X-ray absorption experiments at the Pohang Light Source were supported in part by MOST and POSCO.

References

1. R. Z. Yin, Y. S. Kim, W. U. Choi, S. S. Kim, and H. Kim, *Advances in Quantum Chemistry*, **54**, 23 (2008).
2. W. U. Choi, J. Y. Lee, B. H. Jung, and H. S. Lim, *J. Power Sources*, **136**(1), 154 (2004).
3. T. Zheng, J. S. Xue, and J. R. Dahn, *Chem.Mater.*, **8**, 389 (1996).
4. Sony Lithium Ion Battery Performance Summary, *JEC Batt. Newsletter*, **2**, 31 (1994).
5. S. Levasseur, M. Menetrier, and C. Delmas, *J. Power Sources*, **112**, 419 (2002).
6. M. Zou, M. Yoshio, S. Gopukumar, and J. Yamaki, *Chem. Mater.*, **15**(25), 4699 (2003).
7. H. S. Kim, T. K. Ko, B. K. Na, W. I Cho, and B. W. Chao, *J. Power Sources*, **138**, 232 (2004).
8. M. Mladenova, R. Stoyanovab, E. Zhechevab, and S. Vassilev, *Electro. Comm.*, **3**(8), 410 (2001).
9. J. P. Perdew, K. Burke, and M. Ernzerhof, *Phys. Rev. Lett.*, **77**, 3865 (1996).
10. G. G. Amatucci, J. M. Tarascon, and L. C. Klein, *J. Electrochem. Soc.*, **143**(3), 1114 (1996).
11. Y. M. Kang, Y. I. Kim, M. W. Oh, R. Z. Yin, Y. M. Lee, D. W. Han, H. S. Kwon, J. H. Kim, and G. Ramanath, *Energy & Environ. Sci.*, **4**, 4978, (2011).
12. T. Schultz, S. Zhou, and K. Sundmacher, *Chem. Eng. Technol.*, **24**, 12 (2001).
13. W. Vielstich, A. Lamm, and H. A. Gasteiger (Eds.), *Handbook of Fuel Cells*, vol. 4, John Willey & Sons, New York (2002).
14. Z. Wei, S. Wang, B. Yi, J. Liu, L. Chen, W. Zhou, W. Li, and Q. Xin, *J. Power Sources*, **106**, 364 (2002).
15. A. Lindermeir, G. Rosenthal, U. Kunz, and U. Hoffman, *J. Power Sources*, **129**, 180 (2004).
16. H. Maleki, G. Deng, A. Anani, and J. Howard, *J. Electrochem. Soc.*, **146**, 3224 (1999).